The current issue and full text archive of this journal is available at
**www.emeraldinsight.com/0961-5539.htm**



# On the MHD and slip flow over a rotating disk with heat transfer

Aytac Arikoglu and Ibrahim Ozkol
*Faculty of Aeronautics and Astronautics, Istanbul Technical University, Istanbul, Turkey*

Received October 2004
Revised March 2005
Accepted April 2005


## Abstract

**Purpose** – To study the steady magnetohydrodynamic (MHD) flow of a viscous, Newtonian and electrically conducting fluid over a rotating infinite disk with slip boundary condition.

**Design/methodology/approach** – The governing equations, which are partial and coupled, are transformed to ordinary ones by utilizing the similarity variables introduced by Karman and the resulting equation system is solved by using differential transform method.

**Findings** – It is observed that both the slip factor and the magnetic flux decrease the velocity in all directions and thicken the thermal boundary layer.

**Originality/value** – This paper studies the combined effects of slip and magnetic flux to the flow and thermal fields over a rotating single free disk in an ambient fluid, which were never studied together before.


**Keywords** Rotational motion, Flow, Turbines, Heat transfer

**Paper type** Research paper

## 1. Introduction

The flow due to rotating disks is of great interest in many practical and engineering aspects. Mainly, the requirement for high temperatures in the turbine stage of a gas turbine engine to achieve high thermal efficiencies, the cooling of the air is essential to ensure long lifetime for turbine disks and blades. It is vital to know how the flow and the thermal fields are at every stage for a safe and effective work life, in the operation of the rotary type machine systems. For an accurate determination of temperature distribution, the flow field must be solved as precisely as possible. Since the governing equations, namely the momentum equations, are highly nonlinear and coupled, it is hard to obtain exact analytical solutions for the full problem.

Von Karman (1921), in his pioneering work, discovered the self-similar behavior of the flow over a single free disk and solved the resulting ordinary differential equation system by using an approximate integral method. Later, Cochran (1934) obtained more accurate results by using a Taylor series expansion near the disk, matched with a series solution involving exponentially decaying functions far from the disk at a suitable mid point. Benton (1966) improved Cochran's solutions and solved the problem for the unsteady case. The problem of heat transfer was first considered by Millsaps and Pohlhausen (1952) for the values of Prandtl number (*Pr*) between 0.5 and 10. Later, Sparrow and Gregg (1959) extended this work for a range of $0.1 < Pr < 100$ by neglecting the dissipative terms in the energy equation.

The problem still attracts the attention of researchers from various disciplines, since rotary type flow has many applications in different fields. In more recent studies, the problem is solved for special cases such as presence of second grade (Ariel, 1997),

International Journal of Numerical Methods for Heat & Fluid Flow
Vol. 16 No. 2, 2006
pp. 172-184

0961-5539
DOI 10.1108/09615530610644253

power law (Andersson and de Korte, 2002) or electrically conducting fluids in MHD flow (Takhar *et al.*, 2002) and the cases of suction or injection (Attia, 1998).

Magnetohydrodynamics (MHDs) can be interpreted as a theory of the macroscopic interaction of electrically conducting fluids and electromagnetic fields. Its applications arise in astronomy, space physics and geophysics as well as in connection with many other engineering problems, such as liquid-metal cooling of nuclear reactors, electromagnetic casting of metals, MHD power generation and MHD ion propulsion. Mainly, the most important part of liquid-metal studies is to control the flow of metallic melts since numerous metallurgical processes are governed by MHD effects resulting from the macroscopic interaction of liquid metals with applied or induced currents, electric and magnetic fields.

In this study, the similarity variables introduced by Von Karman (1921) are used with a coordinate stretching technique to solve the set of nonlinear differential equations that define the character of the flow field, in a bounded domain. The resulting differential equation system is solved by differential transform method (DTM). This method was introduced by Zhou (1986) in a study about electrical circuits. It is a semi analytical-numerical technique depending on Taylor series and is promising for the solution of various types of differential equations. With this technique, it is possible to obtain highly accurate results or exact solutions for the differential or integro-differential equation considered (Ayaz, 2004; Arikoglu, 2005).

## 2. Differential transform method

The differential transform of the $k$th derivative of an analytical function $f(x)$ of one variable at $x = x_0$ is as follows:

$$F(k) = \frac{1}{k!}\left[\frac{\mathrm{d}^k f(x)}{\mathrm{d}x^k}\right]_{x=x_0} \tag{1}$$

and the inverse transformation is defined as:

$$f(x) = \sum_{k=0}^{\infty} F(k)(x - x_0)^k \tag{2}$$

Theorems to be used in the transformation procedure, which can be easily evaluated from equations (1) and (2), are given below:

*Theorem 1.* If $f(x) = g(x) \pm h(x)$, then $F(k) = G(k) \pm H(k)$.

*Theorem 2.* If $f(x) = cg(x)$, then $F(k) = cG(k)$, where $c$ is a constant.

*Theorem 3.* If

$$f(x) = \frac{\mathrm{d}^n g(x)}{\mathrm{d}x^n},$$

then

$$F(k) = \frac{(k+n)!}{k!} G(k+n).$$

*Theorem 4.* If $f(x) = g(x)h(x)$, then

$$F(k) = \sum_{l=0}^{k} G(l)H(k-l).$$

*Theorem 5.* If $f(x) = x^n$, then $F(k) = \delta(k-n)$, where $\delta$ is the dirac-delta function that is defined by:

$$\delta(k-n) = \begin{cases} 1 & k = n \\ 0 & k \neq n \end{cases}$$

## 3. Theoretical model

For the MHD flow of an electrically conducting fluid, the conservation of momentum in $r, z$ and $\theta$ directions, the continuity equation and the energy equation, by neglecting the dissipation terms, for steady, incompressible and axially symmetrical case can be written as follows:

$$u\frac{\partial u}{\partial r} + w\frac{\partial u}{\partial z} - \frac{v^2}{r} + \frac{\sigma B_0^2}{\rho}u + \frac{1}{\rho}\frac{\partial p}{\partial r} = \nu\left(\frac{\partial^2 u}{\partial r^2} + \frac{1}{r}\frac{\partial u}{\partial r} - \frac{u}{r^2} + \frac{\partial^2 u}{\partial z^2}\right) \tag{3a}$$

$$u\frac{\partial v}{\partial r} + w\frac{\partial v}{\partial z} + \frac{uv}{r} + \frac{\sigma B_0^2}{\rho}v = \nu\left(\frac{\partial^2 v}{\partial r^2} + \frac{1}{r}\frac{\partial v}{\partial r} - \frac{v}{r^2} + \frac{\partial^2 v}{\partial z^2}\right) \tag{3b}$$

$$u\frac{\partial w}{\partial r} + w\frac{\partial w}{\partial z} + \frac{1}{\rho}\frac{\partial p}{\partial z} = \nu\left(\frac{\partial^2 w}{\partial r^2} + \frac{1}{r}\frac{\partial w}{\partial r} + \frac{\partial^2 w}{\partial z^2}\right) \tag{3c}$$

$$\frac{\partial (ru)}{\partial r} + \frac{\partial (rw)}{\partial z} = 0 \tag{3d}$$

$$\rho c_p\left(u\frac{\partial t}{\partial r} + w\frac{\partial t}{\partial z}\right) - k\frac{\partial^2 t}{\partial z^2} = 0 \tag{3e}$$

where, $u$ is the radial, $v$ is the circumferential and $w$ is the axial component of the velocity, $B_0$ is the magnetic flux density, $\sigma$ is the electrical conductivity, $t$ is the temperature, $p$ is the pressure, $\nu$ is the kinematic viscosity, $\rho$ is the density, $c_p$ is the constant pressure specific heat and $k$ is the thermal conductivity.

When the mean free path of the fluid particles is comparable to the characteristic dimensions of the flow field domain, Navier-Stokes equations break down since the assumption of continuum media fails. In the range $0.1 < Kn < 10$ of Knudsen Number, the high order continuum equations, e.g. Burnett equations should be used. For the range of $0.1 > Kn > 0.001$, no-slip boundary conditions can not be used and should be replaced with the following expression (Gad-el-Hak, 1999):

$$U_t = \frac{2-\eta}{\eta}\lambda\frac{\partial U_t}{\partial n} \tag{4}$$

where $U_t$ is the tangent velocity, $n$ is the normal direction to the wall, $\eta$ is the tangential momentum accommodation coefficient and $\lambda$ is the mean free path. For $Kn < 0.001$, the no-slip boundary condition is valid, therefore, the velocity at the surface is equal to zero. In this study the slip and the no-slip regimes of the Knudsen number that lies in the range $0.1 > Kn > 0$ is considered. By using equation (4), the boundary conditions are introduced as follows:

$$u = \frac{2-\eta}{\eta}\lambda\frac{\partial u}{\partial z}, \quad v = r\Omega + \frac{2-\eta}{\eta}\lambda\frac{\partial v}{\partial z}, \quad w = 0 \text{ at } z = 0 \tag{5a}$$

$$u \to 0, \quad v \to 0 \text{ as } z \to \infty \tag{5b}$$

where $\Omega$ is the angular velocity of the rotating disk. Following Von Karman (1921), we introduce the similarity variables:

$$u = \Omega r F(\zeta), \quad v = \Omega r G(\zeta), \quad w = \sqrt{\Omega\nu}H(\zeta), \quad p = -\rho\Omega\nu P(\zeta) \tag{6}$$

where $\zeta = z\sqrt{\Omega/\nu}$ is the dimensionless coordinate in axial direction. By using equation (6), the governing equations given in (3(a))-(3(d)) simplify to the following ordinary, coupled and nonlinear set of differential equations:

$$F'' = HF' + F^2 - G^2 + \beta F \tag{7a}$$

$$G'' = HG' + 2FG + \beta G \tag{7b}$$

$$P' = HH' - H'' \tag{7c}$$

$$H' = -2F \tag{7d}$$

where $\beta = \sigma B_0^2/\rho\Omega$ is the magnetic interaction number, which represents the ratio between the magnetic force to the fluid inertia force. By assuming that temperature is a function of the axial coordinate only and introducing the dimensionless temperature as $T(\zeta) = (t - t_\infty)/(t_0 - t_\infty)$, where $t_0 = t(0)$ and $t_\infty = t(\infty)$, the energy equation given in (3(e)) reduces to:

$$T'' = Pr\, HT' \tag{8}$$

where $Pr$ is the Prandtl number. The boundary conditions for $T(\zeta)$ are given below:

$$T(0) = 1, \quad T(\infty) = 0 \tag{9}$$

By integrating equation (8) with the condition at $\zeta = 0$, $T(\zeta)$ can be evaluated in terms of the axial part of the velocity field as follows:

$$T(\zeta) = T'(0)\int_0^\zeta e^{Pr\int_0^y H(x)\mathrm{d}x}\,\mathrm{d}y + 1 \tag{10}$$

The value of $T'(0)$ is obtained from the far field boundary condition given in equation (9) as follows:

$$T'(0) = \frac{-1}{\int_0^\infty e^{Pr\int_0^y H(x)\mathrm{d}x}\,\mathrm{d}y} \tag{11}$$

The boundary conditions given in equations (5(a) and 5(b)) are expressed in terms of the similarity variables, given in equation (6), as follows:

$$F(0) = \gamma F'(0), \quad G(0) = 1 + \gamma G'(0), \quad H(0) = 0 \tag{12a}$$

$$F(\infty) = 0, \quad G(\infty) = 0 \tag{12b}$$

where $\gamma = [(2-\eta)\lambda\Omega^{1/2}]/\eta\nu^{1/2}$ is the slip factor. Since DTM is based on Taylor series expansion, the problem essentially requires the matching of two series for the inner and the outer regions of the infinite domain. Solution of such a system of equations requires more effort and computer time, so that we introduce the following coordinate transformation and the dependent variables to solve the problem in a bounded domain:

$$\xi = a^{-\zeta} \tag{13}$$

$$F(\zeta) = \log^2(a)f(\xi), \quad G(\zeta) = \log^2(a)g(\xi), \quad H(\zeta) = \log(a)h(\xi) \tag{14}$$

where $a$ is an arbitrary number. Then, equations (7(a)-7(d)) may be written as follows:

$$\xi^2 f'' = f^2 - g^2 - \xi h f' - \xi f' + \alpha f \tag{15a}$$

$$\xi^2 g'' = 2fg - \xi h g' - \xi g' + \alpha g \tag{15b}$$

$$2f = \xi h' \tag{15c}$$

where $\alpha = \beta/\log^2 a$. The boundary conditions given in equations (12(a) and 12(b)) become:

$$f(1) = -\gamma\log(a)f'(1), \quad g(1) = \log^{-2}(a) - \gamma\log(a)g'(1), \quad h(1) = 0 \tag{16a}$$

$$f(0) = 0, \quad g(0) = 0, \quad h(0) = \alpha - 1 \tag{16b}$$

## 4. The solution

To solve the equation system (15(a)-(c)) with the conditions (16(a) and (b)), we apply DTM at the point $\xi = 0$. By using the theorems 1-5, the following recurrence relations are obtained from equations (15(a)-15(c)):

$$(k^2 - \alpha)\tilde{F}(k) - \sum_{l=0}^{k}\tilde{F}(l)\tilde{F}(k-l) + \sum_{l=0}^{k}\tilde{G}(l)\tilde{G}(k-l) + \sum_{l=0}^{k} l\tilde{F}(l)\tilde{H}(k-l) = 0 \tag{17a}$$

$$(k^2-\alpha)\tilde{G}(k)-2\sum_{l=0}^{k}\tilde{F}(l)\tilde{G}(k-l)+\sum_{l=0}^{k}l\tilde{G}(l)\tilde{H}(k-l)=0 \tag{17b}$$

$$2\tilde{F}(k)-k\tilde{H}(k)=0 \tag{17c}$$

where $k\geq 2$ and $\tilde{F}(k)$, $\tilde{G}(k)$ and $\tilde{H}(k)$ denote the differential transform of $f(\xi)$, $g(\xi)$ and $h(\xi)$, respectively. The boundary conditions in equation (16(b)) are transformed as follows:

$$\tilde{F}(0)=0,\quad \tilde{F}(1)=f_1,\quad \tilde{G}(0)=0,\quad \tilde{G}(1)=g_1,\quad \tilde{H}(0)=\alpha-1 \tag{18}$$

where $f_1$ and $g_1$ denote to $f'(0)$ and $g'(0)$, respectively. By using the recurrence relations (17(a)-17(c)) and the transformed boundary conditions in equation (18), $\tilde{F}(k)$, $\tilde{G}(k)$ and $\tilde{H}(k)$ are evaluated in terms of $f_1$, $g_1$ and $\alpha$ for $k=2,3,\ldots,N$. Following this, the series solutions are obtained from:

$$f(\xi)=\sum_{k=0}^{N}\tilde{F}(k)\xi^k,\quad g(\xi)=\sum_{k=0}^{N}\tilde{G}(k)\xi^k,\quad h(\xi)=\sum_{k=0}^{N}\tilde{H}(k)\xi^k \tag{19}$$

Then, by using the boundary conditions given in equation (16(a)) for $\xi=1$, we evaluated $f_1, g_1$ and $\alpha$ numerically. The solution in series form is obtained in one step, without shooting for the missing boundary conditions. By calculating up to $N=5$, we get:

$$\begin{aligned}f(\xi)=f_1\xi-\frac{f_1^2+g_1^2}{\alpha+2}\xi^2+\frac{3f_1\left(f_1^2+g_1^2\right)}{2(\alpha+2)(\alpha+3)}\xi^3\\-\frac{\left(f_1^2+g_1^2\right)\left[g_1^2+(8\alpha+17)f_1^2\right]}{3(\alpha+2)^2(\alpha+3)(\alpha+4)}\xi^4\\+\frac{5f_1\left(f_1^2+g_1^2\right)\left[(\alpha+13)g_1^2+(25\alpha+61)f_1^2\right]}{24(\alpha+2)^2(\alpha+3)(\alpha+4)(\alpha+5)}\xi^5+\cdots\end{aligned} \tag{20}$$

$$\begin{aligned}g(\xi)=g_1\xi-\frac{g_1\left(f_1^2+g_1^2\right)}{2(\alpha+2)(\alpha+3)}\xi^3+\frac{4f_1g_1\left(f_1^2+g_1^2\right)}{3(\alpha+2)(\alpha+3)(\alpha+4)}\xi^4\\-\frac{g_1\left(f_1^2+g_1^2\right)\left[(\alpha+5)g_1^2+(25\alpha+53)f_1^2\right]}{8(\alpha+2)^2(\alpha+3)(\alpha+4)(\alpha+5)}\xi^5+\cdots\end{aligned} \tag{21}$$

$$h(\xi) = \alpha - 1 + 2f_1\xi - \frac{f_1^2 + g_1^2}{\alpha + 2}\xi^2 + \frac{f_1\left(f_1^2 + g_1^2\right)}{(\alpha + 2)(\alpha + 3)}\xi^3 - \frac{\left(f_1^2 + g_1^2\right)\left[g_1^2 + (8\alpha + 17)f_1^2\right]}{6(\alpha + 2)^2(\alpha + 3)(\alpha + 4)}\xi^4 + \frac{f_1\left(f_1^2 + g_1^2\right)\left[(\alpha + 13)g_1^2 + (25\alpha + 61)f_1^2\right]}{12(\alpha + 2)^2(\alpha + 3)(\alpha + 4)(\alpha + 5)}\xi^5 + \cdots \tag{22}$$

The solutions are given here up to $O(\xi^5)$, however, one can easily obtain terms of higher order. After evaluating $f(\xi)$, $g(\xi)$ and $h(\xi)$, the original functions $F(\zeta)$, $G(\zeta)$ and $H(\zeta)$ are obtained by using equations (13) and (14). Then, by using equations (10) and (11), $T(\zeta)$ is evaluated by numerical integration. If necessary, one can obtain $P(\zeta)$ by integrating equation (7(c)) as follows:

$$P(\zeta) - P_0 = H^2/2 - H' \tag{23}$$

## 5. Results and discussion

In the calculations carried out, to assure a 6-digits of accuracy, it is sufficient to take $N = 35$. As an example, convergence of $a$ for $\gamma = 0$ and $\beta = 0$ versus $N$ is given in Table I.

The primary flow field parameters $F'(0)$, $G'(0)$ and $H(\infty)$ for several values of the slip factor $\gamma$ and for $\beta = 0$ are given in Table II with comparison to that in Miklavcic and Wang (2004). The results are also reported for $\beta = 1$ in Table III with comparison to those of Andersson and Korte (2002) for $\gamma = 0$. The variation of other important

**Table I.** Convergence of $a$ for $\gamma = 0$ and $\beta = 0$

| $N$ | 6 | 10 | 15 | 20 | 25 | 30 | 35 |
|---|---|---|---|---|---|---|---|
| $a$ | 2.458276 | 2.432815 | 2.420212 | 2.421829 | 2.421702 | 2.421710 | 2.421710 |

**Table II.** Variation of the flow field parameters due to $\gamma$ for $\beta = 0$ ($n = 60$)

| | $F'(0)$ | | $-G'(0)$ | | $-H(\infty)$ | |
|---|---|---|---|---|---|---|
| $\gamma$ | Present | Miklavcic | Present | Miklavcic | Present | Miklavcic |
| 0.0 | 0.510232619 | 0.51023262 | 0.615922014 | 0.61592201 | 0.88447411 | 0.8844742 |
| 0.1 | 0.421453639 | 0.42145364 | 0.605835241 | 0.60583524 | 0.88136423 | 0.8813642 |
| 0.2 | 0.352581007 | 0.35258101 | 0.583676764 | 0.58367676 | 0.87395729 | 0.8739572 |
| 0.5 | 0.223848209 | 0.22384821 | 0.502809702 | 0.50280970 | 0.84239263 | 0.8423926 |
| 1.0 | 0.127923645 | 0.12792364 | 0.394927595 | 0.39492760 | 0.78947720 | 0.7894772 |
| 2.0 | 0.061010098 | 0.06101010 | 0.273370132 | 0.27337013 | 0.71031331 | 0.7103134 |
| 5.0 | 0.018588527 | 0.01858853 | 0.143388209 | 0.14338821 | 0.58376463 | 0.5837646 |
| 10.0 | 0.006812558 | 0.00681256 | 0.081030089 | 0.08103009 | 0.48758465 | 0.4875846 |
| 20.0 | 0.002361594 | 0.00236159 | 0.043788462 | 0.04378846 | 0.39997581 | 0.3999758 |

parameters $T'(0), f_1, g_1$ and $a$ with the slip factor $\gamma$ are given in Tables III and V for $\beta = 0$ and $\beta = 1$, respectively.

For these calculations we took $Pr = 0.71$, which is the value of Prandtl number for air. By continuing the same procedure, the thermal field can be computed for different Prandtl numbers. One can deduce from equation (23) that $P(\infty)$ is related to the axial velocity at infinity as $P(\infty) - P_0 = H(\infty)^2/2 - 2F(0)$. If necessary, one can obtain $P(\infty)$ by using the values given in Tables II and IV for $H(\infty)$ and $F'(0)$, knowing that the slip velocity on the surface is related to the skin friction as $F(0) = \gamma F'(0)$ (Table V).

| $\gamma$ | $F'(0)$ Present | $F'(0)$ Andersson | $-G'(0)$ Present | $-G'(0)$ Andersson | $-H(\infty)$ Present | $-H(\infty)$ Andersson |
|---|---|---|---|---|---|---|
| 0.0 | 0.3092580 | 0.3093 | 1.0690534 | 1.0691 | 0.2533143 | 0.2533 |
| 0.1 | 0.2275672 | – | 0.9730532 | – | 0.2478159 | – |
| 0.2 | 0.1727037 | – | 0.8881437 | – | 0.2360560 | – |
| 0.5 | 0.0869394 | – | 0.6979959 | – | 0.1938269 | – |
| 1.0 | 0.0370585 | – | 0.5130955 | – | 0.1376430 | – |
| 2.0 | 0.0113924 | – | 0.3366878 | – | 0.0767438 | – |
| 5.0 | 0.0014983 | – | 0.1669337 | – | 0.0237061 | – |
| 10.0 | 0.0002479 | – | 0.0909351 | – | 0.0076573 | – |
| 20.0 | 0.0000359 | – | 0.0476211 | – | 0.0021867 | – |

**Table III.** Variation of the flow field parameters due to $\gamma$ for $\beta = 1$ ($n = 40$)

| $\gamma$ | $-T'(0)$ | $f_1$ | $g_1$ | $a$ |
|---|---|---|---|---|
| 0.0 | 0.325860639 | 1.182244779 | 1.536776526 | 2.421710504 |
| 0.1 | 0.333496950 | 1.096913972 | 1.422174786 | 2.414190968 |
| 0.2 | 0.336780900 | 1.038943086 | 1.339504645 | 2.396375269 |
| 0.5 | 0.334652873 | 0.942790947 | 1.191324451 | 2.321915819 |
| 1.0 | 0.320432993 | 0.875499819 | 1.076800290 | 2.202244788 |
| 2.0 | 0.292997980 | 0.825074692 | 0.983003210 | 2.034628635 |
| 5.0 | 0.244046155 | 0.783417800 | 0.898674732 | 1.792774875 |
| 10.0 | 0.205049245 | 0.765039980 | 0.858998126 | 1.628378368 |
| 20.0 | 0.168829630 | 0.753582150 | 0.833355187 | 1.491788616 |

**Table IV.** Variation of $T'(0), f_1$ and $g_1$ with respect to $\gamma$ for $\beta = 0$ ($n = 60$)

| $\gamma$ | $-T'(0)$ | $f_1$ | $g_1$ | $a$ |
|---|---|---|---|---|
| 0.0 | 0.1466260 | 0.2295591 | 0.8003710 | 3.1100731 |
| 0.1 | 0.1454969 | 0.2059028 | 0.7224999 | 3.1004750 |
| 0.2 | 0.1404346 | 0.1861206 | 0.6633721 | 3.0801221 |
| 0.5 | 0.1192323 | 0.1419627 | 0.5438620 | 3.0089722 |
| 1.0 | 0.0880740 | 0.0969619 | 0.4278653 | 2.9188418 |
| 2.0 | 0.0515184 | 0.0529581 | 0.3037245 | 2.8266939 |
| 5.0 | 0.0202761 | 0.0161282 | 0.1616369 | 2.7508867 |
| 10.0 | 0.0128822 | 0.0051699 | 0.0899881 | 2.7287291 |
| 20.0 | 0.0107770 | 0.0014684 | 0.0474785 | 2.7212572 |

**Table V.** Variation of $T'(0), f_1$ and $g_1$ with respect to $\gamma$ for $\beta = 1$ ($n = 40$)

As it is seen from Figure 1, the wall gradient in radial direction monotonically decreases with $\beta$ and $\gamma$.

Figure 2 shows that as $\gamma$ increases, the magnitude of the velocity gradient in circumferential direction decreases. This is a consequence that the fluid cannot stick on the rotating disk; therefore, the slipping fluid decreases the surface skin friction. Since $G(\zeta)$ inevitably has to change from $G(0)$ at the surface of the disk to zero at infinity, an increase in $\beta$, which has a thinning effect on the circumferential boundary layer, leads to an increase of the magnitude of $G'(0)$, for any value of $\gamma$.

Figure 3 shows that, while the heat transfer from the disk, which is directly related to the magnitude of the dimensionless temperature gradient at the surface, monotonically decreases with $\beta$, the variation of $T'(0)$ with the slip factor is more subtle. For $\beta \neq 0$, the magnitude of $T'(0)$ monotonically decreases with $\gamma$ and for $\beta = 0$ it increases up to $\gamma = 0.2836$ taking its maximum value, which is $T'(0) = -0.337462$ and then decreases. We can state that the maximum cooling of the rotating

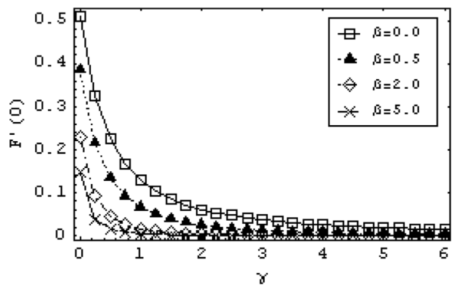


**Figure 1.**
Variation of $F'(0)$ with $\gamma$ for several values of $\beta$

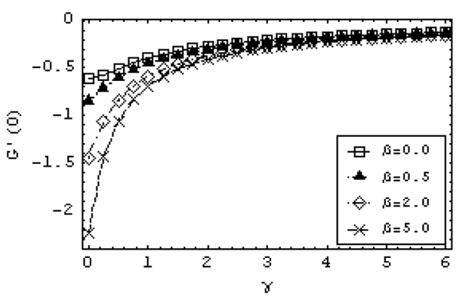


**Figure 2.**
Variation of $G'(0)$ with $\gamma$ for several values of $\beta$

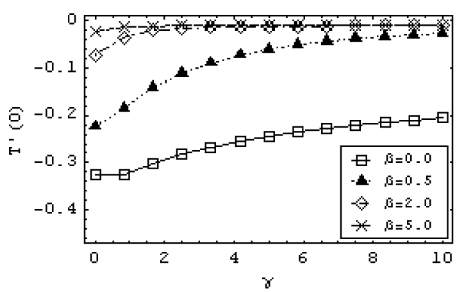


**Figure 3.**
Variation of $T'(0)$ with $\gamma$ for several values of $\beta$

disk is reached at this value of the slip factor if the ambient fluid is colder than the rotating disk surface.

The inflow rate at infinity, as one can see from Figure 4, decreases both with the slip factor and the magnetic interaction number. This is quite natural since the radially outwards boundary layer is fed by the axial flow at infinity.

The highest value of the radial velocity on the surface is 0.128440 and this value is reached at $\gamma = 1.1586$ and $\beta = 0$. This value of the slip factor may be necessary and important in practical applications, when the aim is to use the disk as a centrifugal fan (Figure 5). As one can see from Figure 6, the maximum circumferential velocity on the surface is at $\gamma = 0$, where the no-slip condition is present. This is a result of the negative gradient of the circumferential velocity in $z$ direction above the disk. Variations of the radial velocity $F$ and the temperature $T$ for several values of $\gamma$ and $\beta$ are given in Figures 7 and 8.

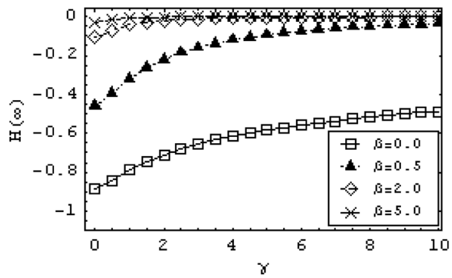


**Figure 4.**
Variation of $H(\infty)$ with $\gamma$ for several values of $\beta$

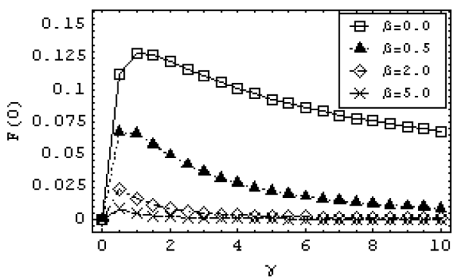


**Figure 5.**
Variation of $F(0)$ with $\gamma$ for several values of $\beta$

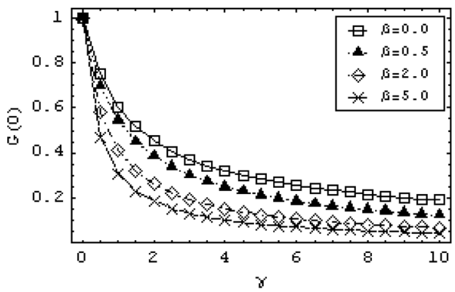


**Figure 6.**
Variation of $G(0)$ with $\gamma$ for several values of $\beta$

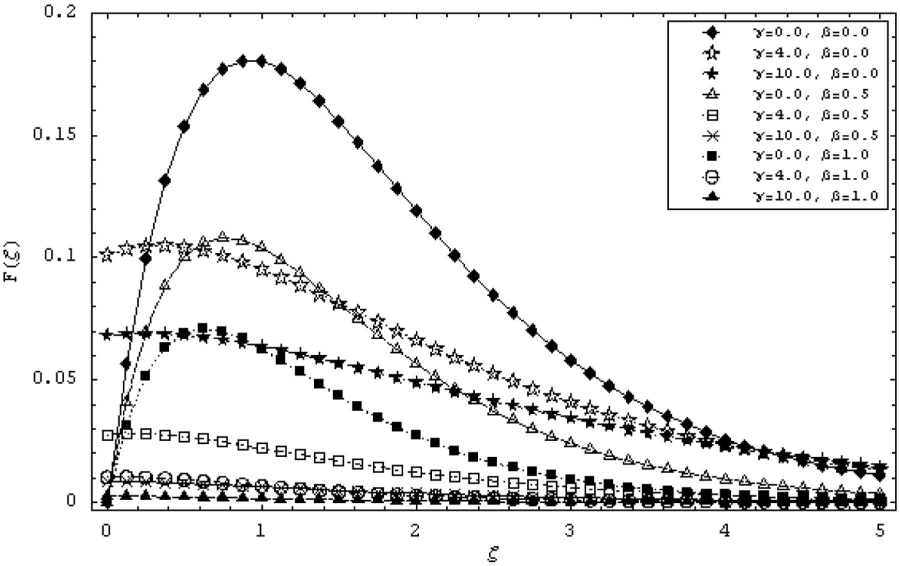


**Figure 7.**
Radial component of the velocity for several values of $\gamma$ and $\beta$

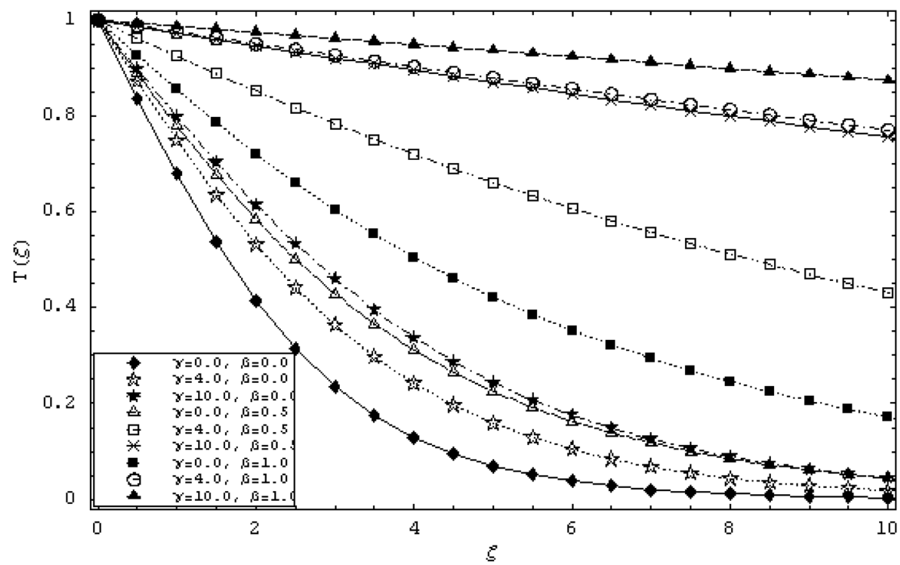


**Figure 8.**
Variation of temperature for several values of $\gamma$ and $\beta$, $Pr = 0.71$

In Figure 7, the decreasing effect of the slip factor $\gamma$ on radial boundary layer can be seen. In the limit case $\gamma \rightarrow \infty$, when the flow is entirely potential, the rotating disk has no effect to rotate the fluid particles, therefore, the fluid is at rest. This is quite natural, since the rotating disk acts like a centrifugal fan and owing to the centrifugal forces, throws out the fluid that sticks to it. A fluid stream compensates this thrown fluid, which is in the axial direction. When $\gamma$ increases, less amount of fluid can stick to the disk and the rotating disk loses its efficiency to transfer its circumferential momentum to the fluid particles. The fluid loses circumferential velocity, leading the centrifugal force that throws the fluid outwards to decrease. When the disk throws less fluid outwards, less amount of fluid stream in the axial direction exists.

The effect of the magnetic field is to reduce, and eventually suppress the radial outflow. An accompanying reduction of the axial flow together with a thinning of the circumferential boundary layer, which leads to an increase in the wall gradient that causes in an increase of the torque required to turn the disk, can be observed.

In Figure 8, one can observe that as the slip factor increases, $T(\zeta)$ tends to vary linearly. This is a result of the fact that as $\gamma$ increases, $H(\zeta)$ decreases and in the limit case of $\gamma \rightarrow \infty$, $H = 0$ can be taken. From equation (8), this leads to the following case:

$$\lim_{\gamma \rightarrow \infty} T''(\zeta) = 0 \tag{24}$$

where the solution is linear and for large values of $\gamma$, it can be approximated as: $T(\zeta) \cong T'(0)\zeta + 1$ to ease the computations. Also the magnetic interaction number $\beta$ and the slip factor $\gamma$ have thickening effects on the thermal boundary layer.

## 6. Conclusion

In this study, the magnetic effects to an electrically conducting fluid in slip regime are studied for the flow field on a single rotating disk with heat transfer. A coordinate stretching method is used to solve the problem in a bounded domain and DTM, which is a versatile tool for solving non-linear partial or ordinary differential equations, is used as the solution technique. The flow field variables are obtained in series form. The combined effects of the slip factor $\gamma$ and the magnetic interaction number $\beta$ are studied in detail.

## References

Andersson, H.I. and de Korte, E. (2002), "MHD flow of a power law fluid over a rotating disk", *European J. Mech. B/Fluids*, Vol. 21, pp. 317-24.

Ariel, P.D. (1997), "Computation of flow of a second grade fluid near a rotating disk", *Int. J. Engng Sci.*, Vol. 35, pp. 1335-57.

Arikoglu, A. and Ozkol, I. (2005), "Solution of boundary value problems for integro-differential equations by using differential transform method", *Appl. Math. Comput.* Vol. 168, pp. 1145-58.

Attia, H.A. (1998), "Unsteady MHD flow near a rotating porous disk with uniform suction or injection", *Fluid Dyn. Res.*, Vol. 23, pp. 283-90.

Ayaz, F. (2004), "Solutions of the system of differential equations by differential transform method", *Appl. Math. Comput.*, Vol. 147, pp. 547-67.

Benton, E.R. (1966), "On the flow due to a rotating disk", *J. Fluid Mech.*, Vol. 24, pp. 781-800.

Cochran, W.G. (1934), "The flow due to a rotating disc", *Proc. Cambridge Phil. Soc.*, Vol. 30, pp. 365-75.

Gad-el-Hak, M. (1999), "The fluid mechanics of microdevices – the Freeman Scholar Lecture", *J. Fluid Eng-T. Asme*, Vol. 121, pp. 5-33.

Miklavcic, M. and Wang, C.Y. (2004), "The flow due to a rough rotating disk", *Z. Angew. Math. Phys.*, Vol. 55, pp. 235-46.

Millsaps, K. and Pohlhausen, K. (1952), "Heat transfer by laminar flow from a rotating plate", *J. Aero. Sci.*, Vol. 19, pp. 120-6.

Sparrow, E.M. and Gregg, J.L. (1959), "Heat transfer form a rotating disk to fluids of any Prandtl number", *J. Heat Tran., Trans. ASME*, Vol. 81, pp. 249-51.

Takhar, H.S., Singh, A.K. and Nath, G. (2002), "Unsteady MHD flow and heat transfer on a rotating disk in an ambient fluid", *Int. J. Therm. Sci.*, Vol. 41, pp. 147-55.

Von Karman, T. (1921), "Über laminare und turbulente reibung", *Z. Angew. Math. Mech.*, Vol. 1, pp. 233-52.

Zhou, J.K. (1986), *Differential Transformation and its Application for Electrical Circuits*, Huazhong University Press, Wuhan.

## Further reading

Bird, G.A. (1996), *Molecular Gas Dynamics and the Direct Simulation of Gas Flows*, Oxford University Press, Oxford.

## Corresponding author

Ibrahim Ozkol is the corresponding author and can be contacted at: ozkol@itu.edu.tr